

A status report of the QCDSF $N_f=2+1$ Project

Meinulf Göckeler^a, Roger Horsley^b, Yoshifumi Nakamura^{*,c}, Holger Perlt^d, Dirk Pleiter^c, Paul E. L. Rakow^e, Gerrit Schierholz^{c,f}, Arwed Schiller^d, Thomas Streuer^g, Hinnerk Stüben^h and James M. Zanotti^b

^a *Institut für Theoretische Physik, Universität Regensburg, 93040 Regensburg, Germany*

^b *School of Physics, University of Edinburgh, Edinburgh EH9 3JZ, UK*

^c *John von Neumann Institute NIC / DESY Zeuthen, 15738 Zeuthen, Germany*

^d *Institut für Theoretische Physik, Universität Leipzig, 04109 Leipzig, Germany*

^e *Department of Mathematical Sciences, University of Liverpool, Liverpool L69 3BX, UK*

^f *Deutsches Elektronen-Synchrotron DESY, 22603 Hamburg, Germany*

^g *Department of Physics and Astronomy, University of Kentucky, Lexington KY 40506, USA*

^h *Konrad-Zuse-Zentrum für Informationstechnik Berlin, 14195 Berlin, Germany*

E-mail: yoshifumi.nakamura@desy.de

QCDSF Collaboration

We report about on-going simulations of $N_f=2+1$ lattice QCD. We use a tadpole improved Symanzik gauge action and stout link smeared Wilson fermions with a clover term. We employ the Hasenbusch trick for the degenerate u- and d-quarks, and the RHMC algorithm for the simulation of the strange quark.

XXVth International Symposium on Lattice Field Theory

July 30- August 4, 2007

University of Regensburg, Germany

*Speaker.

1. Introduction

Over the past few years the QCDSF Collaboration has focused on simulations of lattice QCD with 2 flavors of dynamical quarks. The real world consists, however, of $N_f=2+1$ light quarks (up, down and strange). We therefore extend our previous simulations to $N_f=2+1$ where we continue to investigate hadron and quark masses, weak matrix element, hadron form factors, moments of parton distributions as well as a variety of other key parameters of the Standard Model. Our ultimate goal is to bring the systematic uncertainties down to or below the experimental errors.

JLQCD found an unexpected first-order phase transition in the strong coupling regime at relatively heavy quark masses when they employed the plaquette gauge action and the $O(a)$ -improved Wilson fermion action in three-flavor QCD simulations [1]. Using an improved gauge action should give us significantly better control on the continuum extrapolation. Additionally, it is important to reduce somehow the chiral symmetry breaking arising from the Wilson fermion formulation. A well-known method to attenuate this symmetry breaking is adding a clover term. The *UV filtering* method, which involves replacing covariant derivatives in the fermion action by smeared descendents, is also becoming standard. We employ a tadpole improved Symanzik gauge action and stout link smeared Wilson fermions with a clover term. We also improve the algorithm to reduce simulation costs.

2. The Action

The tadpole-improved Symanzik action we use for $N_f=2+1$ simulations is

$$S_G = \frac{6}{g^2} \left[c_0 \sum_{\text{plaquette}} \frac{1}{3} \text{Re Tr}(1 - U_{\text{plaquette}}) + c_1 \sum_{\text{rectangle}} \frac{1}{3} \text{Re Tr}(1 - U_{\text{rectangle}}) \right], \quad (2.1)$$

where the coefficients c_0, c_1 are taken from tadpole improved perturbation theory:

$$\frac{c_1}{c_0} = -\frac{1}{20u_0^2}, \quad (2.2)$$

with $c_0 + 8c_1 = 1$, where $u_0 = \left(\frac{1}{3} \text{Tr} \langle U_{\text{plaquette}} \rangle\right)^{\frac{1}{4}}$. We write $\beta = \frac{6}{g^2} c_0$. In the classical continuum limit $u_0 \rightarrow 1$ the coefficients assume the tree-level Symanzik values [2] $c_0 = 5/3, c_1 = -1/12$.

We continue to use clover fermions with the action

$$S_F = \sum_x \left\{ \bar{\psi}(x) \psi(x) - \kappa \bar{\psi}(x) U_\mu^\dagger(x - \hat{\mu}) [1 + \gamma_\mu] \psi(x - \hat{\mu}) \right. \\ \left. - \kappa \bar{\psi}(x) U_\mu(x) [1 - \gamma_\mu] \psi(x + \hat{\mu}) + \frac{i}{2} \kappa c_{\text{SW}} \bar{\psi}(x) \sigma_{\mu\nu} F_{\mu\nu}(x) \psi(x) \right\}, \quad (2.3)$$

but replace the gauge links U_μ in all terms of the fermion action except the clover term by stout links [3]

$$U_\mu \rightarrow \tilde{U}_\mu(x) = e^{iQ_\mu(x)} U_\mu(x), \quad (2.4)$$

with

$$Q_\mu(x) = \frac{\alpha}{2i} \left[V_\mu(x) U_\mu^\dagger(x) - U_\mu(x) V_\mu^\dagger(x) - \frac{1}{3} \text{Tr} \left(V_\mu(x) U_\mu^\dagger(x) - U_\mu(x) V_\mu^\dagger(x) \right) \right], \quad (2.5)$$

where $V_\mu(x)$ is the sum over all staples associated with the link. We take $\alpha = 0.1$ and perform 1 level of smearing, corresponding to a mild form of *UV filtering* [4]. In this status report we present results where we used the tree-level value for the improvement coefficient, i.e. $c_{\text{SW}} = 1$, or used a value obtained from tadpole-improved perturbation theory:

$$c_{\text{SW}} = \frac{1}{u_0^3} [1 + g^2(0.00706281 + 1.142004\alpha - 4.194470\alpha^2)], \quad g^2 = \frac{6}{\beta} \frac{20u_0^2}{20u_0^2 - 8}. \quad (2.6)$$

Note that in the future we will use the results presented in [5].

This action has many advantages over our previously used one. In particular, due to *UV filtering*, it is expected to have better chiral properties [6] and smaller cut-off effects [7]. One may also hope that the tadpole-improved perturbative value of c_{SW} is close to the non-perturbative value.

3. The Algorithm

The standard partition function for $N_f=2+1$ improved Wilson fermions is

$$Z = \int DUD\bar{\psi}D\psi e^{-S}, \quad (3.1)$$

$$S = S_g(\beta) + S_l(\kappa_l, c_{\text{SW}}) + S_s(\kappa_s, c_{\text{SW}}),$$

where S_g is a gluonic action, S_l is an action for the degenerate u- and d- quarks and S_s is an action for the strange quark. After integrating out fermions

$$S = S_g(\beta) - \ln[\det M_l^\dagger M_l][\det M_s^\dagger M_s]^{\frac{1}{2}}. \quad (3.2)$$

We first apply even-odd preconditioning:

$$\det M_l^\dagger M_l \propto \det(1 + T_{oo}^l)^2 \det Q_l^\dagger Q_l, \quad [\det M_s^\dagger M_s]^{\frac{1}{2}} \propto \det(1 + T_{oo}^s)[\det Q_s^\dagger Q_s]^{\frac{1}{2}}, \quad (3.3)$$

where

$$Q = (1 + T)_{ee} - M_{eo}(1 + T)_{oo}^{-1} M_{oe}, \quad T = \frac{i}{2} c_{\text{SW}} \kappa \sigma_{\mu\nu} F_{\mu\nu}. \quad (3.4)$$

We then separate $\det Q_l^\dagger Q_l$ following Hasenbusch [8]

$$\det Q_l^\dagger Q_l = \det W_l^\dagger W_l \det \frac{Q_l^\dagger Q_l}{W_l W_l^\dagger}, \quad W = Q + \rho. \quad (3.5)$$

Finally we modify the standard action to

$$S = S_g + S_{det}^l + S_{det}^s + S_{f1}^l + S_{f2}^l + S_{fr}^s, \quad (3.6)$$

where

$$S_{det}^l = -2 \text{Tr} \log[1 + T_{oo}(\kappa^l)], \quad S_{det}^s = -\text{Tr} \log[1 + T_{oo}(\kappa^s)],$$

$$S_{f1}^l = \phi_1^\dagger [W(\kappa^l)^\dagger W(\kappa^l)]^{-1} \phi_1, \quad S_{f2}^l = \phi_2^\dagger W(\kappa^l) [Q(\kappa^l)^\dagger Q(\kappa^l)]^{-1} W(\kappa^l)^\dagger \phi_2,$$

$$S_{fr}^s = \sum_{i=1}^n \phi_{2+i}^\dagger [Q(\kappa^s)^\dagger Q(\kappa^s)]^{-\frac{1}{2n}} \phi_{2+i}. \quad (3.7)$$

We calculate S_{fr} using the RHMC algorithm [9] with optimized values for n and the number of fractions. We now split each term of the action into one ultraviolet and two infrared parts,

$$S_{UV} = S_g, \quad S_{IR-1} = S_{det}^l + S_{det}^s + S_{f1}^l, \quad S_{IR-2} = S_{f2}^l + S_{fr}^s. \quad (3.8)$$

In [10] we have introduced two different time scales [11] for the ultraviolet and infrared parts of the action in the leap-frog integrator. Here we shall go a step further and put S_{UV} , S_{IR-1} and S_{IR-2} on *three separate* time scales,

$$\begin{aligned} V(\tau) &= \left[V_{IR-2} \left(\frac{\delta\tau}{2} \right) A^{m_1} V_{IR-2} \left(\frac{\delta\tau}{2} \right) \right]^{n_\tau}, \\ A &= V_{IR-1} \left(\frac{\delta\tau}{2m_1} \right) B^{m_2} V_{IR-1} \left(\frac{\delta\tau}{2m_1} \right), \\ B &= V_{UV} \left(\frac{\delta\tau}{2m_1 m_2} \right) V_Q \left(\frac{\delta\tau}{m_1 m_2} \right) V_{UV} \left(\frac{\delta\tau}{2m_1 m_2} \right), \end{aligned} \quad (3.9)$$

where $n_\tau = \tau/(\delta\tau)$ and the V s are evolution operators of the Hamiltonian. The length of the trajectory τ is taken to be equal to one in our simulations.

4. Test calculations

We first tested our algorithm on small lattices of size 4^4 and 8^4 . Figure 1 shows the acceptance ratio and $e^{-\Delta H}$ for $\beta = 7.2$, $\kappa_l = \kappa_s = 0.1245$ and $c_{SW} = 1.0$ for various simulation parameters. We discarded for thermalisation the first 200 trajectories and then calculated for each choice of the simulation parameters about 1000 trajectories. $e^{-\Delta H}$ should be equal to one within error and this is a good indicator of the correctness of the program. As seen in Fig. 1, we can keep high acceptance and $e^{-\Delta H} \approx 1$ by tuning parameters. Simulation results for the same parameters on a $16^3 \times 32$ lattice

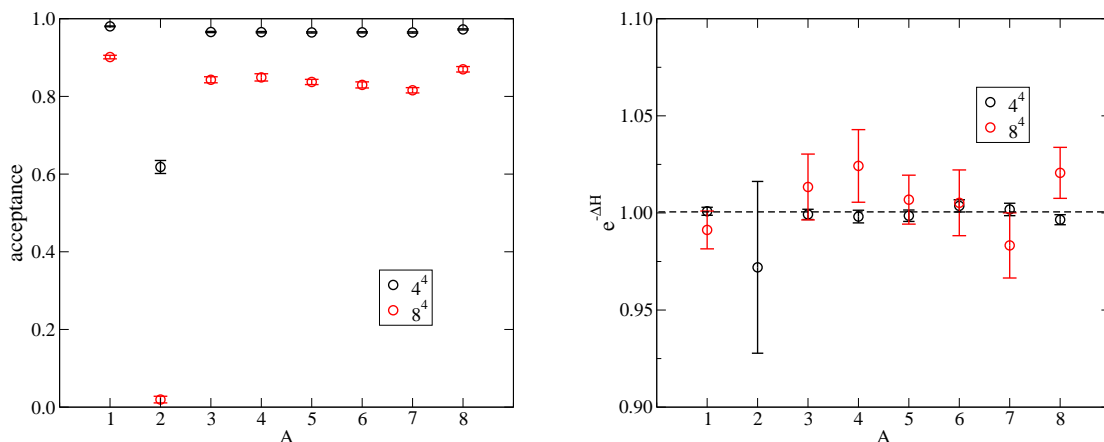


Figure 1: The acceptance (left) and $e^{-\Delta H}$ (right) for various simulation parameters. $A: (m_1, m_2, \rho) = (3, 3, 0.1), (1, 1, 0.1), (2, 2, 0.1), (2, 2, 0.2), (2, 2, 0.3), (2, 2, 0.4), (2, 2, 0.5), (3, 3, 0.5)$. The other simulation parameters are fixed to $n_\tau = 20$, CG residual for Monte Carlo $res_{mc} = 10^{-10}$, CG residual for Molecular Dynamics $res_{md} = 10^{-7}$ and the rational approximation by $n=2$, 20 fractions and range $[0.01, 3]$.

are presented in table 1. The lattice spacing roughly corresponds to the so-called *fine* run of the

MILC collaboration [12] which is using the same gauge action. Figure 2 is a plot of κ_c^V , which is obtained by extrapolating the valence pion mass to zero, as a function of $(r_0 m_{PS})^2$. We see that κ_c^V for $N_f=2+1$ is lower than for $N_f=2$. Assuming that κ_c^V also has a rather mild β dependence, we may consider this as an indication that our new action is much more continuum like.

r_0/a	am_{PS}	am_V	am_N	κ_c^V
4.89(15)	0.9089(20)	0.9520(25)	1.4828(53)	0.134599(63)

Table 1: r_0/a , m_{PS} , m_V , m_N and κ_c^V obtained from partially quenched calculations on a $16^3 32$ lattice for $\beta = 7.2$, $\kappa_l = \kappa_s = 0.1245$ and $c_{SW} = 1.0$.

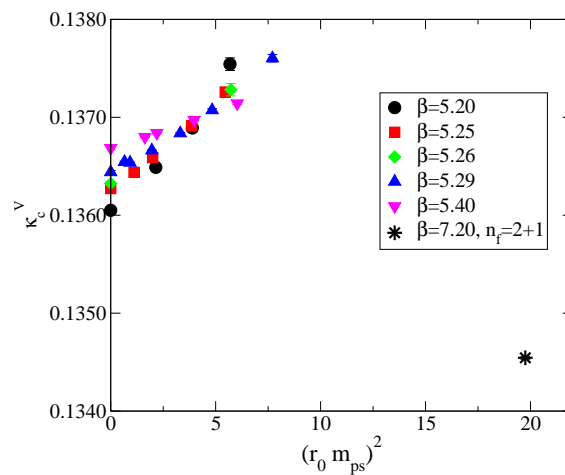


Figure 2: κ_c^V versus $(r_0 m_{PS})^2$ at $\beta = 5.2 \sim 5.4$ for $N_f=2$ and at $\beta = 7.2$ for $N_f=2+1$.

Results for $\beta = 7.2$, $\kappa_l = \kappa_s = 0.1335$ with tadpole improved c_{SW} on a $16^3 32$ lattice are presented in table 2. They were calculated from 200 trajectories varying n of eq. (3.7), the number of fractions and the precision of the coefficients for the rational approximation. Our results confirm that double precision coefficients are needed to obtain the correct value of $e^{-\Delta H}$. Note that the average plaquette value as well as the average minimum and maximum eigenvalue are consistent for the different choices of the algorithmic parameters. But since S_{fr} may be $O(10^8)$ (e.g. on large lattices) the algorithm may not be correct when using single precision coefficients. For the parameters shown in the last row of table 2, the ratios for the force contributions from the different terms in the action are

$$\frac{F_{det_l}}{F_{det_s}} = 2, \quad \frac{F_{f1}}{F_{det_s}} \sim 30, \quad \frac{F_{f2}}{F_{det_s}} \sim 10, \quad \frac{F_{fr}}{F_{det_s}} \sim 10, \quad \frac{F_g}{F_{det_s}} \sim 90. \quad (4.1)$$

F_{fr} for $n=4$ is 40% smaller than for $n=2$.

5. Conclusion

In this contribution we have presented the status of our $N_f=2+1$ project. We found indications for our action to be better than our previously used action. Furthermore, we tested the correctness of our algorithm. The performance of our program for matrix multiplication is about 20% of the

n	fr.	pr.	P	τ_{int}	$e^{-\Delta H}$	P_{acc}	λ_{min}	λ_{max}
2	32	s	0.625591(55)	2.07(76)	1.167(25)	0.96	0.011247(64)	2.4788(44)
4	40	s	0.625578(52)	2.10(85)	1.529(24)	0.99	0.011306(62)	2.4757(40)
2	32	d	0.625528(41)	1.74(46)	0.995(17)	0.91	0.011316(66)	2.4805(33)

Table 2: Simulation parameters and results for the value of the plaquette, the integrated autocorrelation time of the plaquette, $e^{-\Delta H}$, acceptance, minimum and maximum eigenvalues of $Q^\dagger Q$ on a 16^3 32 lattice for $\beta = 7.2$, $\kappa_l = \kappa_s = 0.1335$ and tadpole improved $c_{SW}=1.612$. The parameters are the number n of eq. (3.7), the number of fractions (fr.) and the precision of the coefficients for the rational approximation (pr.). The other parameters are fixed to $n_\tau=60$, $m_1=3$, $m_2=3$, $res_{mc}=10^{-10}$, $res_{md}=10^{-8}$ and $\rho=0.1$.

peak performance on the SGI Altix 4700. We are planning to implement better integration schemes and test other separations, for instance,

$$S_{UV} = S_g, \quad S_{IR-1} = S_{f1}^l, \quad S_{IR-2} = S_{f2}^l + S_{fr}^s + S_{det}^s + S_{det}^l. \quad (5.1)$$

Acknowledgments

The numerical calculations have been performed on the SGI Altix 4700 at LRZ (Munich), as well as on the APEmille at DESY (Zeuthen). We thank all institutions. This work has been supported in part by the EU Integrated Infrastructure Initiative Hadron Physics (I3HP) under contract number RII3-CT-2004-506078 and by the DFG under contract FOR 465 (Forschergruppe Gitter-Hadronen-Phänomenologie).

References

- [1] S. Aoki *et al.*, Phys. Rev. **D72** (2004) 054510 [hep-lat/0409016].
- [2] K. Symanzik, Nucl. Phys. **B226** (1983) 187.
- [3] C. Morningstar and M. J. Peardon, Phys. Rev. **D69** (2004) 054501 [hep-lat/0311018].
- [4] S. Capitani, S. Dürr and C. Hoelbling, JHEP 0611 (2006) 028 [hep-lat/0607006].
- [5] H. Perlt *et al.* [QCDSF Collaboration], PoS(LATTICE 2007)250 [arXiv:0710.0990].
- [6] S. Boinepalli *et al.*, Phys. Lett. **B616** (2005) 196 [hep-lat/0405026].
- [7] J.M.Zanotti *et al.*, Phys. Rev. **D71** (2005) 034510 [hep-lat/0405015].
- [8] M. Hasenbusch, Phys. Lett. **B519** (2001) 177 [hep-lat/0107019].
- [9] M. A. Clark and A. D. Kennedy, Nucl. Phys. Proc. Suppl., **129** (2004) 850 [hep-lat/0309084].
- [10] A. Ali Khan *et al.*, Phys. Lett. **B564** (2003) 235 [hep-lat/0303026].
- [11] J. C. Sexton and D. H. Weingarten, Nucl. Phys. **B380** (1992) 665.
- [12] C. Aubin *et al.*, Phys. Rev. **D70** (2004) 094505 [hep-lat/0402030].